The effects of thermal annealing on the obliquely deposited Ag–Ge–S thin films

F. Wang [a], W.P. Dunn [b], M. Jain [b], C. De Leo [b], N. Vicker [b], R. Savage [b], X. Jin [b], S. Mamedov [c], P. Boolchand [d]

[a] *EE Department, California State University, Long Beach, CA 90840, USA*
[b] *College of Engineering, California Polytechnic State University, San Luis Obispo, CA 93407*
[c] *HORIBA Jobin Yvon Inc., Edison, NJ 08820*
[d] *ECE Department, University of Cincinnati, Cincinnati, OH 45221*

A B S T R A C T

Obliquely deposited thin films of ternary Ag–Ge–S glasses are characterized in this work. Thin films are fabricated in a vacuum thermal evaporator at different evaporation angles and examined by Raman spectroscopy. The Raman mode frequency of GeS_4 corner-sharing (CS) structure of the as-deposited films display a red-shift as a function of Ag content due to reduced global connectivity, and therefore decreased network stress. Film thickness of normally deposited thin films is significantly less when compared against obliquely deposited ones. Sulfur-ring (S_8) modes are observed in thin films but not in corresponding bulk material. Thermal annealing of thin films results in the disappearance of Sulfur-ring (S_8) modes, while the temperature required for this phenomenon is deposition angle dependent. Thickness of the obliquely deposited films shrinks significantly after thermal annealing, which indicates a collapse of the micro-column structure introduced by oblique deposition.

1. Introduction

Chalcogenide glasses are extensively used in rewritable non-volatile memory applications. In general, non-volatile memory devices based on chalcogenide materials could be categorized into two types. One is information storage based on the phase change of chalcogenide materials between an amorphous state and a crystalline state [1]. This technique is widely used in rewritable optical data recordings (e.g. RW-DVD discs). Materials used as active recording layers for this category are Sb–Te containing alloys, with the most widely used material being the Ge–Sb–Te (GST) system [2–4]. This type of non-volatile memory is known as phase change memory (PCM).

The other type of information storage mechanism is relatively new. It is known as Programmable Metallization Cell (PMC) memory. This type of memory device controls the forming and dissolving of metal conduction links in a solid state electrolyte through electrochemical methods [5,6]. The resistance switching between the two states is used for binary data recording purpose. Materials used as active recording media for this category are chalcogenides containing super ionic metals, such as Ag–Se, Ag–S [7], Ag–Ge–Se [5,6], Ag–Ge–S [8], Cu–S [9], etc. PMC devices, compared to phase change memory, has the advantages of shorter recording time, lower recording power and better scaling capability [5,6].

Silver germanium sulfide (Ag–Ge–S) films have demonstrated PMC behavior, and several successful devices have been fabricated [7,8]. In general, the fabrication process plays a significant role in term of thin films' structure and network stress, and thus affects the PMC behavior of the thin films. Therefore, to improve the yield of PMC devices, one needs to have a thorough knowledge of the thin film's characteristics, such as its molecular structure and network stress, under different fabrication conditions.

The aim of this work is to study: (1) the structure of Ag–Ge–S thin films deposited at different deposition angles and (2) the effects of thermal annealing to the structure of those films. The thin films are prepared using vacuum thermal evaporation methods and characterized using Raman spectroscopy.

2. Experiment

Ternary Ag–Ge–S glasses with composition $Ag_x(Ge_{25}S_{75})_{1-x}$ ($x = 0.1$ and 0.2) are synthesized by mixing a measured amount of Ag mesh (99.999%), Ge shots (99.999%) and Sulfur chips (99.999%) in a vacuumed quartz tubing. The quartz tubes are pumped down to 10^{-7} Torr and sealed before being placed into a furnace. The temperature is then slowly (1 °C/min) increased to 950 °C. The melts are homogenized at 950 °C for 2–3 days before the temperature is reduced down to 600 °C. Samples are water

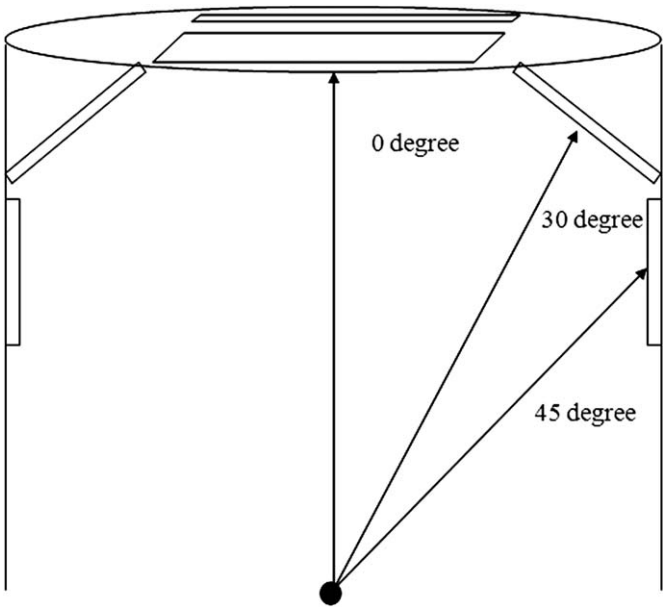

Fig. 1. Substrate layout in bell jar. The substrates placed on top of the bell jar are considered normal deposition (0°), the substrates placed at the corner have a deposition angle of 30° and the substrates placed on the side wall have a deposition angle of 45°.

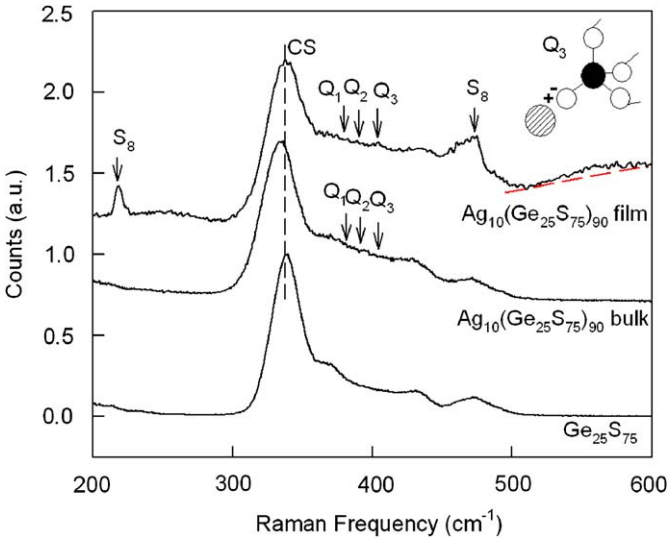

Fig. 2. Raman results of $Ag_x(Ge_{25}S_{75})_{1-x}$ ($x = 10\%$) thin film, $Ag_x(Ge_{25}S_{75})_{1-x}$ ($x = 10\%$) bulk and $Ge_{25}S_{75}$ bulk [10,11]. The Raman line-shapes of both thin film and bulk reveal corner sharing (CS) tetrahedral modes, edge-sharing (ES) modes and Thiogemanate modes (Q_1–Q_3). Raman line-shape of thin film also reveals modes for S_8 rings located at 220 and 470 cm^{-1}. $Ge_{25}S_{75}$ Raman result is also displayed for comparison purpose.

quenched after being homogenized at 600 °C for at least 12 h. Bulk sample synthesis is completed at the Solid State Physics and Electronic Materials Lab at the University of Cincinnati, Ohio.

Thin films are fabricated using a Varian VE-10 vacuum evaporator. Freshly quenched samples are aged in quartz tubes for 2 months before being evaporated. This allows sufficient time for glasses to age to a saturated state. The bulk materials are then powdered and loaded into evaporation boats. We covered the evaporation boats using a fine tungsten mesh in order to avoid spitting during the evaporation process. Glass substrates are placed at 0°, 30° and 45° locations, respectively, as shown in Fig. 1.

As-deposited thin films are separated into three groups. The first group contains virgin films without any further process. The second group of thin films is thermally annealed at 150 °C for 1 h. The third group of films is thermally annealed at 200 °C for 1 h. In the following text, we will call them Group 1 (virgin), Group 2 (150 °C annealed) and Group 3 (200 °C annealed), respectively. Raman spectroscopy of thin films from all three groups are obtained. (Raman experiments are done in Horiba Jobin Yvon Inc. New Jersey location). The Raman spectra of the films are obtained using a He–Ne laser (632.8 nm) focused through a 100× objective. The optical power at the sample is 0.6 mW. The thicknesses of the evaporated thin films from all three groups are measured using a profiliometer.

3. Results and discussion

3.1. Normally deposited films

Fig. 2 shows the Raman line-shapes obtained from thin-films of $Ag_x(Ge_{25}S_{75})_{1-x}$ ($x = 10\%$), corresponding bulk material and bulk $Ge_{25}S_{75}$, respectively [10,11]. The Raman results from the thin films qualitatively agree with that of the corresponding bulk materials. In both thin films and bulk, the Raman results clearly show corner-sharing (CS) Ge-S_4 tetrahedra (~340 cm^{-1}), edge-sharing (ES) Ge-S_4 tetrahedra (~360 cm^{-1}) and thio-germanate units Q_m, $m = 1,2,3$ (~370, 390 and 405 cm^{-1}, respectively). The existence of thio-germanate units in thin films is verified by comparing Raman line-shape of thin film $Ag_x(Ge_{25}S_{75})_{1-x}$ ($x = 10\%$) with that of $Ge_{25}S_{75}$ [12]. The Raman of $Ge_{25}S_{75}$ shows a deep valley between 370 and 420 cm^{-1}, while that of $Ag_x(Ge_{25}S_{75})_{1-x}$ ($x = 10\%$) thin film is flat, which indicates some additional modes in that region. Thio-germanate units (Q_m units) are clear signs of Ag mingling within the atomic lattice. This indicates a successful deposition of Ag–Ge–S thin films using thermal evaporation method. Here, m represents the number of bridging sulfur in the units. The inset in Fig. 2 gives an illustration for the Q_3 units. This unit has 3 bridging sulfurs and 1 terminating sulfur attached by an Ag atom. Q_1 and Q_2 units may be deduced by analogy.

Besides the similarity, there are also some discrepancies between the Raman spectra of thin films and those of the bulk. First of all, sharp peaks are observed at 220 and 470 cm^{-1} in the thin film but not in the bulk. These peaks are known to correspond to S_8 rings. Second, one should notice that, for thin film samples, there is a significant blue shift in CS mode frequency, compared to that of the corresponding bulk sample. According to Cai and Boolchand [15], the CS mode frequency in Ge_xS_{1-x} system blue shifts as a function of x, i.e., as the backbone becomes sulfur deficient. The same phenomenon is observed in Ge_xSe_{1-x} as well [16,17]. The Raman results indicate that S_8 rings monomers are segregated from the backbone network. In $Ag_x(Ge_{25}S_{75})_{1-x}$ thin films, this segregation will leave the backbone network (mainly tetrahedral centered at Ge atoms) sulfur deficient. This explains the blue shift observed in the Raman of thin films. Our interpretation to the sulfur segregation in thin film is mainly due to the low vaporization temperature of sulfur (57 °C). During the evaporation, a small amount of sulfur is vaporized earlier than Ag and Ge.

Fig. 3 compares the $Ag_x(Ge_{25}S_{75})_{1-x}$ thin films of 10% and 20%. The CS mode frequency of 20% film is red shifted compared to that of the 10% film. Similar red shifts are observed in bulk $Ag_x(Ge_{25}S_{75})_{1-x}$ materials as well [10,11]. There is more than one mechanism that can cause Raman mode frequency to red shift. According to F. Wang's work on bulk Ag–Ge–S [11,12], when Ag enters the Ge–S network, some attach to the Ge–S tetrahedral to form thio-germanate units (Q_1, Q_2 or Q_3); the rest form Ag_2S

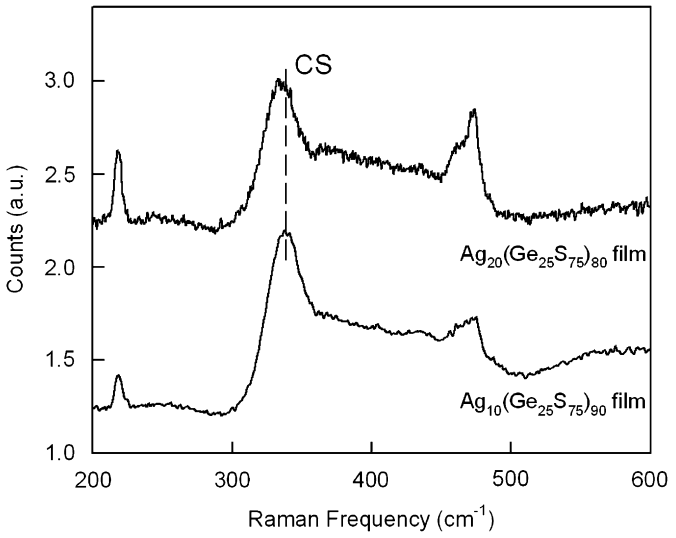

Fig. 3. Raman line-shapes of normally deposited thin film $Ag_x(Ge_{25}S_{75})_{1-x}$ ($x = 10\%$ and 20%). CS mode frequency red-shifts as x increases.

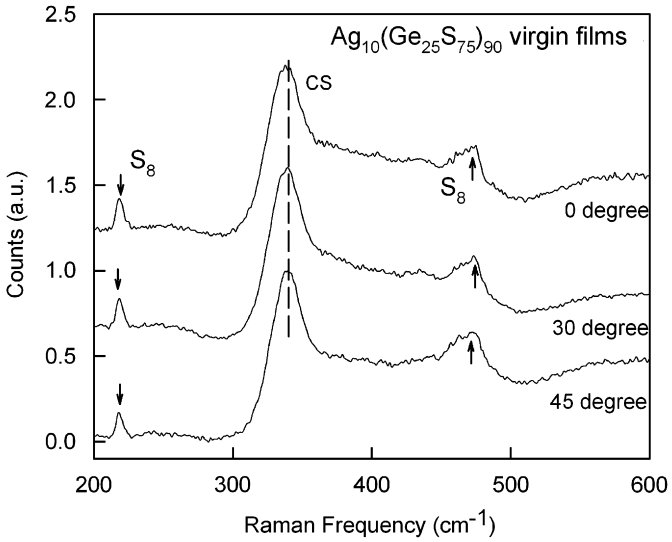

Fig. 4. Raman results from the as-deposited thin films at 0° (normal deposition), 30° and 45°.

structures that segregate from the backbone network. Therefore, $Ag_x(Ge_{25}S_{75})_{1-x}$ glasses are intrinsically phase-separated. From network stress point of view, it does not matter whether Ag is forming Ag_2S monomers or thio-germanate units; the ultimate effect is reduced network connectivity. In the Ge–S backbone, sulfur atoms serve as bridges. Attaching an Ag atom to a bridging sulfur atom basically cuts that bridge, thus, makes it terminate. This reduces the overall network connectivity of backbone. Obviously, forming Ag_2S also reduces the backbone's connectivity since Ag steals a bridging S from the backbone, resulting in a monomer that does not connect to the backbone. Lower connectivity results in less network stress, which appears in the Raman spectra as a red shift. As the Ag content increases, both Ag_2S segregation and thio-germanate unit formations increase. Therefore, one should expect less network stress in 20% of $Ag_x(Ge_{25}S_{75})_{1-x}$ than that in 10%. On the other hand, bond defects and lattice disorder also result in red-shifts in the Raman spectra [13,14]. When Ag atoms attach to Ge-S_4 tetrahedra, it will introduce more bond disorder due to the oversized Ag-ion, which could also result in red shifts in the Raman spectra. More silver atoms are involved in 20% film than 10% film, therefore, one expects more bond disorder in 20% film.

3.2. Obliquely deposited thin films

The Raman results of thin films from group 1 (virgin films) are shown in Fig. 4. Qualitatively, the Raman results of thin films deposited at all three angles coincide with each other. Peakfit (AISN Software Inc.) is utilized to de-convolute the Raman line-shapes into a combination of Gaussian peaks. Fig. 5 illustrates a sample fitting of virgin thin films of 10% $Ag_x(Ge_{25}S_{75})_{1-x}$ deposited at 30°. The full width half maximum (FHWM) of CS modes shows a decreasing trend from 0° to 45°, while a slight red-shift in the peak center is observed (see Table 1). Line-widths of Raman scattering are well accepted as a measure of disorder in glassy lattices, which in turn results in a red-shift in mode frequencies. Our results show that normal deposition (0°) introduces more significant bond disorder. This is probably because the atoms in a vapor are normally bombarding onto substrates, which will likely result in defects in bonds.

Also in Table 1, the thickness measurements of thin films at all three degrees are listed (the values in Table 1 are average of 6 films from the same batch). The thicknesses of normally deposited

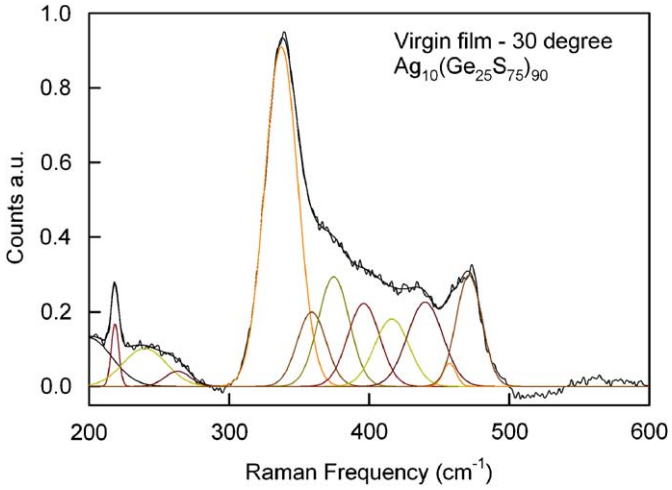

Fig. 5. Sample fitting using Peakfit (AISN Software Inc.) of 10% $Ag_x(Ge_{25}S_{75})_{1-x}$ virgin thin film deposited at 30°.

Table 1
Comparison of Raman spectroscopy and thickness measurements for three deposition angles.

	CS Center (cm^{-1})	CS FHWM (cm^{-1})	CS Intensity	Thickness (nm)
0°	336.13	28.54	0.86	192
30°	337.74	27.74	0.91	246
45°	337.95	26.22	0.833	251

thin films are significantly smaller than those of obliquely deposited ones. This could be partially due to the larger bombarding energy produced during the film deposition process in a normal deposition setup. In addition, obliquely deposited thin films usually show columnar structure inclining towards the substrate. As the deposition angle increases, spacing starts to form between columns due to shadowing effects. This results in large amount of void areas between columns [18]. Paritosh and Srolovitz [18] show that shadowing effect starts to introduce

voids when the deposition angle (α) is greater than 20°. The existence of voids must enlarge the overall volume of the film. This further explains the significant thickness difference between the normally deposited thin films (191 nm) and the obliquely deposited ones (246 and 251 nm).

3.3. Thermal annealing effects

Raman line-shapes of thin films from group 2 (annealed at 150 °C for 1 h) and group 3 (annealed at 200 °C for 1 h) are displayed in Fig. 6. After 150 °C annealing for 1 h, one clearly observes the disappearance of modes at 220 cm^{-1} from Raman results (mode corresponds to S_8 rings) in 45° films. This indicates that the S_8 rings are decomposed. While in 30° films, the intensity of this mode is significantly reduced, but not completely decomposed. The intensity of the S_8 ring mode in normally deposited films (0°) remains constant after 150 °C annealing. After 200 °C annealing for 1 h (group 3), the S_8 ring modes completely decomposed from all three angles. The Raman mode at 470 cm^{-1} (high frequency modes due to S_8 rings) shows similar trends as the 220 cm^{-1} mode.

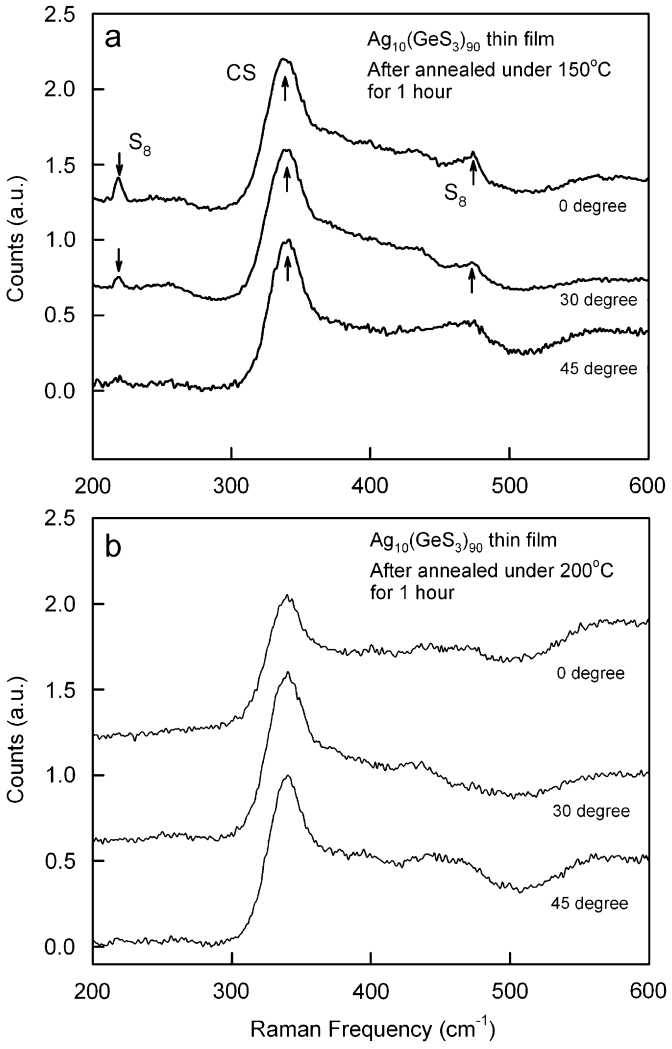

Fig. 6. (a) Raman results from obliquely deposited thin films after annealing under 150 °C for 1 h and (b) Raman results from obliquely deposited thin films after annealing under 200 °C for 1 h.

This temperature dependence is mostly due to the columnar structure of obliquely deposited films. As explained in previous section, significant voids in volume start to build up starting from 20° deposition angle. These voids not only expand the volume of the films, but also increase the effective surface of the films. The loose packing nature of the obliquely deposited films facilitates the decomposition of S_8 rings in thin films. Thickness measurements of post-annealed thin films further supports the columnar structure assumption. After being annealed under 150 °C, the thickness of films deposited at 0°, 30° and 45° shrinks 12.5%, 19% and 44%, respectively. The huge condensation for 45° films retraces to the softening of the micro-columnar structures and, therefore, filling of the voids in the film.

4. Conclusions

$Ag_x(Ge_{25}S_{75})_{1-x}$ ($x = 10\%$ and 20%) thin films are fabricated using a vacuum thermal evaporation method at three different deposition angles (0°, 30° and 45°). Raman spectroscopy results show that the molecular structure of the thin films qualitatively agree with those produced by the corresponding bulk materials except that S_8 ring modes are observed in thin films but not in bulk. This is because of the low vaporization temperature of sulfur, which forces a small amount of sulfur to vaporize earlier than Ag or Ge. Raman and thickness measurements of obliquely deposited thin films proved that normally deposited films have more bond disorder than obliquely deposited ones. Also, obliquely deposited thin films have more voids in their structure due to the shadowing effects. The significant voids in obliquely deposited thin films reduce the packing density and increase the effective surface of those films. Therefore, under thermal annealing, we observe that Raman modes of S_8 rings decomposed at a much lower temperature from obliquely deposited films than from normally deposited ones.

Acknowledgments

This work was sponsored by the Department of the Navy, Office of Naval Research, under Award # N00014-06-1-1111.

References

[1] S.R. Ovshingsky, Phys. Rev. Lett. 21 (1968) 1450.
[2] T. Ohta, J. Optoelectron. Adv. Mater. 3 (2001) 609.
[3] J. Siegel, A. Schropp, J. Solis, C.N. Afonso, M. Wuttig, Appl. Phys. Lett. 84 (2004) 2250.
[4] T. Ohta, E.R. Ovshynsky, in: A.V. Kolobov (Ed.), Photo-Induced Metastavility in Amorphous Semiconductors, Wiley-VCH, Weinheim, 2003, p. 310.
[5] M.N. Kozicki, M. Yun, S.J. Yang, J.P. Aberouette, J.P. Bird, Superlattices Microstructures 27 (2000) 485–488.
[6] M.N. Kozicki, C. Gopalan, M. Balakrishnan, M. Park, M. Mitkova, Non-Volatile Mem. Technol. Symp. Proc. (2004) 15–17.
[7] I. Chaitanya, et al., Presentation at American Physical Society March Meeting, Baltimore, MD, 2006, unpublished.
[8] Carter De Leo, Senior Project Report, California Polytechnic State University, 2007.
[9] T. Sakamoto, H. Sunamura, H. Kawaura, T. Hasegawa, T. Nakayama, M. Aono, Appl. Phys. Lett. 82 (2003) 3032.
[10] P. Boolchand, Fei Wang, Uday Vempati, in: Presentation at American Physical Society March Meeting, Montreal, Canada, 2004, unpublished.
[11] Fei Wang, M. Mitkova, P. Boolchand, in: Presentation at the 22nd International Conference on Amorphous and Nanocrystalline Semiconductors, Denver, Colorado, 2007, unpublished.
[12] Fei Wang, Ph.D. Thesis, University of Cincinnati, 2005.
[13] M.X. Gu, L.K. Pan, B.K. Tay, Chang Q. Sun, J. Raman Spectrosc. 38 (2007) 780–788.
[14] M. Stabl, L. Ticky, Solid State Sci. 7 (2005) 201–207.
[15] L. Cai, P. Boolchand, Philos. Mag. B 82 (2002) 1649.
[16] X. Feng, W.J. Bresser, P. Boolchand, Phys. Rev. Lett. 78 (1997) 4422.
[17] F. Wang, S. Mamedov, P. Boolchand, B. Goodman, M. Chandrasekhar, Phys. Rev. B 71 (2005) 174201.
[18] Paritosh, D.J. Srolovitz, J. Appl. Phys. 91 (4) (2001) 1963–1972.